Europace Advance Access published September 8, 2011

Europace
doi:10.1093/europace/eur284

CLINICAL RESEARCH

Sufficient pulmonary vein image quality of non-enhanced multi-detector row computed tomography for pulmonary vein isolation by catheter ablation

Hirosuke Yamaji[1], Kazuyoshi Hina[1], Hiroshi Kawamura[1], Takashi Murakami[1], Masaaki Murakami[1], Satoshi Hirohata[1], Natsuki Ohmaru[2], and Shozo Kusachi[2]*

[1]Section of Heart Rhythm Center, Okayama Heart Clinic, 54-1,Takeda, Naka-ku, Okayama 700-8251, Japan; and [2]Department of Medical Technology, Okayama University Graduate School of Health Sciences, 2-5-1 Shikata-cho, Kita-ku, Okayama 700-8558, Japan

Received 28 January 2011; accepted after revision 4 August 2011

Aims We evaluated the quality of non-enhanced multi-detector row computed tomography (MDCT) images of the pulmonary vein (PV) and the clinical results of catheter ablation to isolate the PV for treatment of atrial fibrillation (AF) without the use of contrast medium in patients with chronic kidney disease (CKD).

Methods and results We compared PV images quantitatively and qualitatively between non-enhanced and enhanced images ($n = 50$). Procedural parameters and clinical outcomes were compared between catheter ablation for AF referring solely to non-enhanced MDCT in CKD patients ($n = 20$) and using enhanced MDCT images integrated with electroanatomic mapping in non-CKD patients ($n = 30$). In gross anatomy, complete agreement was obtained between non-enhanced and enhanced MDCT images. Bland–Altman plots and cumulative coefficient variation showed good agreement in PV diameter determination between non-enhanced and enhanced MDCT images. There were no statistically significant differences in procedural or fluoroscopic times between PV isolation only referring to non-enhanced MDCT images and that using enhanced MDCT images integrated with electroanatomic mapping. Similarly, the ablation success rate and AF-free status at 3 months after PV isolation did not differ between PV isolation referring only to non-enhanced MDCT images and that using an electroanatomic integration system. No complications occurred in PV isolation with or without enhanced MDCT.

Conclusions Non-enhanced MDCT provides adequate PV image quality both quantitatively and qualitatively. The present study suggests that catheter ablation referring solely to non-enhanced MDCT images for AF could be performed with clinically acceptable results. These findings warrant further studies involving a much larger number of patients to confirm the present results.

Keywords Pulmonary vein • Contrast medium • Creatinine • Radiologic examination

Introduction

Radiofrequency (RF) energy applied to circumferentially isolate the pulmonary veins (PVs) from the left atrium (LA; PV isolation) has been introduced for the treatment of atrial fibrillation (AF) and has shown a cure rate in the range of 50–90%.[1–6]

Precise knowledge of the anatomy of the PVs, in addition to that of the LA, is essential to increase the successful rate of PV isolation, decrease complications, and shorten the time required for the isolation. As PV anatomy demonstrates considerable variation,[7] multi-detector row computed tomography (MDCT) with contrast medium, that is, enhanced MDCT, is now routinely applied to assess PV and LA anatomy.[8] Furthermore, the use of enhanced MDCT images integrated with an electroanatomic map, known as the electroanatomic integration system, is now routinely applied in PV isolation.[9,10] However, it is well known that contrast medium

* Corresponding author. Tel: +81 86 235 6897; fax: +81 86 222 7768, Email: shokus0110@yahoo.co.jp

affects renal function at various degrees and/or evokes an allergic response in certain patients. Thus, MDCT cannot be applied in patients with renal insufficiency or allergies to contrast medium.

Recent MDCT systems have an increased number of detector rows, and consequently MDCT with 64 detector rows has high spatial and time resolution power. We hypothesized that MDCT without using contrast medium, that is, non-enhanced MDCT, would provide sufficient image quality of PV anatomy for PV isolation. In this study, we first compared PV image quality between non-enhanced and enhanced MDCT in patients who underwent PV isolation for the treatment of AF. Secondly, the procedural parameters and clinical outcomes of PV isolation referring solely to non-enhanced MDCT images in patients with CKD were compared with those obtained using enhanced MDCT images integrated with an electroanatomical map in non-CKD patients.

Patients and methods

First, we compared images obtained by non-enhanced and enhanced MDCT in 50 consecutive patients 1–2 days before PV isolation for AF in patients without disturbed renal function. Next, we performed PV isolation referring solely to non-enhanced MDCT in 20 patients with CKD and compared the procedural parameters and clinical outcomes with those from 30 non-CKD patients who underwent PV isolation using enhanced MDCT images integrated with an electroanatomic map during almost the same period. The characteristics of the patients studied are summarized in *Table 1*. The examination procedure complied with the rules of the Helsinki Declaration;[11] written informed consent was obtained; and the study was approved by our institutional ethics committee for human research.

Multi-detector row computed tomography

Scan protocol

Multi-detector row computed tomography was performed with a 64-detector slice computed tomography system (Aquilion 64, Toshiba Medical System, Toshiba, Otawara, Japan). Before enhanced MDCT, a non-enhanced MDCT scan was performed without prospective ECG-triggering to establish the conditions and settings for enhanced MDCT. Computed tomography started at the top of the lung cavity and stopped at the diaphragm caudally. The CT acquisition parameters were collimation thickness, 0.5–1.0 mm; pitch, 0.84 mm; rotation time, 400–500 ms; tube voltage, 120–135 kV; and tube current, 300–400 mA. Scanning was automatically started 5 s after detection of the CT value of 150 HU at the ascending aorta. Images were collected in the supine position. Acquisition was ECG-non-gated and took 7–10 s. After the non-enhanced image was acquired, enhanced MDCT was performed. A non-ionic contrast medium (370 mg/mL, iodine) of 80 mL was administered through the antecubital vein with a power injector at a rate of 2.5 mL/s.

Image reconstruction

For both non-enhanced and enhanced MDCT, transverse PV images were reconstructed using the standard built-in ECG-gated half or multisector scan reconstruction algorithm (temporal resolution, 200–250 ms; slice thickness, 0.5 mm; and increment, 0.3 mm). Pulmonary vein images were reconstructed using volume rendering and multiplanar reconstruction methods. Pulmonary vein images were analysed using an offline workstation for post-processing (ZIO STATION, AMIN Corporation, Tokyo, Japan) to check the main anatomic landmarks by multiplanar reformation.

Table 1 Patient characteristics

Patients for comparison of non-enhanced and enhanced MDCT images			
Number of patients	50		
Age (years)	63 ± 8		
Male (%)	64		
Hypertension (%)	42		
Diabetes (%)	24		
Coronary artery disease (%)	6		
Heart failure (%)	2		
Left atrial size (mm)	42 ± 7		
LVEF (%)	63 ± 8		
Paroxysmal/non-paroxysmal AF	38:12		
Patients with and without CKD who underwent PV isolation			
	CKD(+) group	CKD(−) group	
Number of patients	20	30	NS
Age (years)	58 ± 8	57 ± 9	NS
Male (%)	70%	71%	NS
Cr (mg/dL)	2.09 ± 0.24	0.78 ± 0.19	<0.01
Hypertension (%)	44%	39%	NS
Diabetes (%)	36%	31%	NS
Coronary artery disease (%)	14%	12%	NS
Heart failure (%)	15%	13%	NS
Left atrial size (mm)	41 ± 4	39 ± 5	NS
LVEF (%)	61 ± 9	63 ± 8	NS
Paroxysmal/non-paroxysmal AF	16:4	24:6	NS

PV, pulmonary vein; CKD, chronic kidney disease; MDCT, multi-detector computed tomography; 3D, three dimensional; Cr, creatinine; LVEF, left ventricular ejection fraction; AF, atrial fibrillation

Multi-detector row computed tomography image interpretation

Evaluation of MDCT images was performed by two radiological technicians who were not aware of any clinical data. The three-dimensional image was rotated in space such that the PV and its ostium were visualized completely. The ostial transverse and antero-posterior diameters of PVs were measured with digital calipers (*Figure 1*). Before comparison of PV diameter between non-enhanced and enhanced MDCT images, inter- and intra-observer differences were checked in 50 sample PV images. Then the average of two measurements of PV diameter by each observer was obtained. The median of averaged diameters derived from the two observers was used for analysis. We compared the diameters of PVs obtained by non-enhanced and enhanced MDCT images.

Catheter ablation for atrial fibrillation

Electrophysiological study

Two standard electrophysiology catheters were positioned: a 4-F catheter (Japan Lifeline Co., Ltd., Tokyo, Japan) at the His bundle region via a femoral vein and a 6-F catheter in the coronary sinus via the right intrajugular vein. An 8.5-F steerable sheath (Agilis, St Jude Medical

Inc., St Paul, MN, USA) was advanced to the LA by the Brockenbrough technique under intracardiac echo (ICE; Ultra ICE, Boston Scientific, San Jose, CA, USA) guidance: all sheaths were over one puncture site. After transseptal catheterization, intravenous heparin was administered to maintain an activated clotting time of 300–350 s. In addition, continuous infusion with heparinized saline was connected to the transseptal sheaths (flow rate of 10 mL/h) to avoid thrombus formation or air embolism. Two 20-polar ring catheters (Libero, Japan Lifeline Co. Ltd.) were positioned at the ostia of the PVs. An ablation catheter (CoolPath Duo, St Jude Medical Inc.) was also introduced into the LA.

Creation of three-dimensional geometry of the left atrium and four pulmonary veins

A non-fluoroscopic navigation system (Ensite NavX^{TM}, St Jude Medical) was used to create a three-dimensional (3D) map of the PVs with the LA and to perform PV isolation.

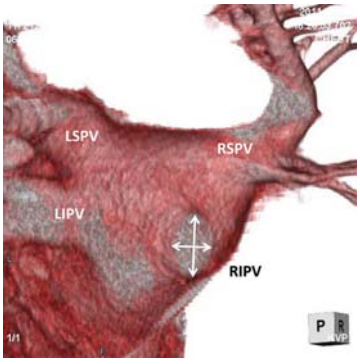

Figure 1 Measurement of pulmonary vein diameter in images obtained from non-enhanced multi-detector row computed tomography using digital calipers at the ostium of the pulmonary vein. LSPV, left superior pulmonary vein; LIPV, left inferior pulmonary vein; RSPV, right superior pulmonary vein; RIPV, right inferior pulmonary vein.

In the CKD patients, first a non-enhanced MDCT image of the PVs and LA was displayed on one of the side monitors. The positional relationships between the four PVs and LA were confirmed using the non-enhanced MDCT image. Then, using the NavX system, the 3D geometry of the four PVs was systematically created with a 20-polar ring catheter, referring to the non-enhanced MDCT image (*Figure 2*). All PV geometry was obtained using the pullback manoeuvre from distal to proximal PV. At least 300 points that synchronized with the catheter tracing were taken to visualize the PV orifice during electroanatomical mapping by the NavX system. Tracing of the catheter tip on the body and appendage of the LA was performed to construct the LA geometry. In each procedure, to create the 3D geometry of the four PVs and LA, non-enhanced MDCT images, rotating appropriately, were referred to in order to confirm the accordance of the 3D geometry generated by NavX with the non-enhanced LA–PV image. Thereafter, referring to the non-enhanced MDCT images carefully, the ostia of the PVs were identified electrophysiologically using the 20-polar ring catheter and ablation catheter positioned at the ostium of each PV under the guidance of ICE, and the correct ablation site then marked on the electroanatomic map (*Figure 3*). The 3D PV geometry derived using the NavX system was not able to fuse with the preprocedural non-enhanced MDCT image.

CKD patients, using contrast medium, selective PV venography was performed. The ostia of the PVs were identified using electrophysiological study results combined with PV venography findings. The 20-polar ring catheter and ablation catheter were then used to determine the mitral annulus and all PV ostia and these points were tagged on the electroanatomic map. Finally, the 3D-LA geometry was fused with the preprocedural enhanced CT images to confirm the correct position of the ablation catheter for PV isolation.

Pulmonary vein isolation

If patients were in AF at the time of the procedure, they underwent external electrical cardioversion before ablation. Two 20-polar ring catheters (Japan Lifeline Co. Ltd.) were placed within the ipsilateral superior and inferior PVs or within the superior and inferior branches of a common trunk PV during RF delivery. Irrigated RF energy was delivered with a target temperature of 42°C, a maximum power limit of 35 W, and an infusion rate of 13 mL/min for the CoolPath DuoTM catheter. Radiofrequency energy was applied for 30 s until

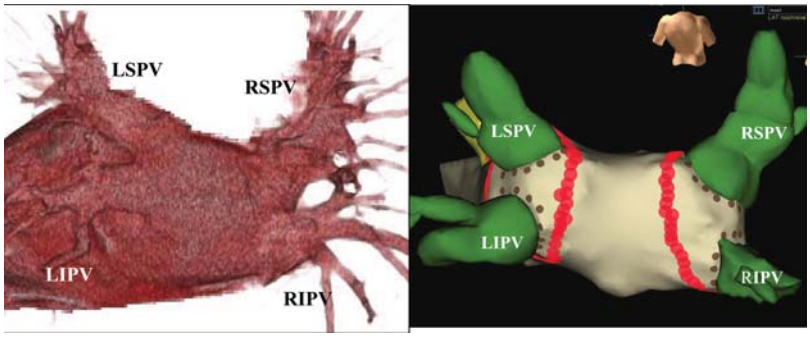

Figure 2 Correspondence between a multi-detector row computed tomography image (left side) and the image created by the non-fluoroscopic navigation system (NavX) (right side). Both images are the same postero-anterior projection view. The brown dots indicate the ostium of each pulmonary vein. The red dots indicate ablation lesions. LSPV, left superior pulmonary vein; LIPV, left inferior pulmonary vein; RSPV, right superior pulmonary vein; RIPV, right inferior pulmonary vein.

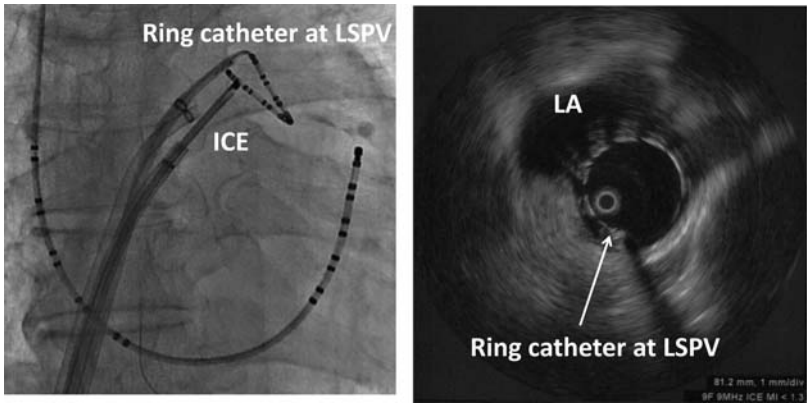

Figure 3 Correct positioning of the ablation catheter for pulmonary vein isolation using an intracardiac echocardiogram (ICE) as the guide. The antero-posterior fluoroscopic image (left side) shows the position of the ICE catheter and ring catheter at the ostium of the left superior pulmonary vein (LSPV). LA, left atrium. ICE image (right side) demonstrates ICE guidance to position the ring catheter at the ostium of the pulmonary vein. The ring catheter can be seen at the ostium of the LSPV.

Table 2 Comparison of pulmonary vein gross anatomy and pulmonary vein diameter between enhanced and non-enhanced multi-detector row computed tomography

Gross anatomy	Observer 1	Observer 2	Agreement rate	Agreement rate		
	Non-enhanced MDCT vs. enhanced MDCT	Non-enhanced MDCT vs. enhanced MDCT	Observer 1 vs. Observer 2	Non-enhanced MDCT vs. enhanced MDCT		
Normal PV	42/42	42/42	100%	100%		
Left common trunk PV	5/5	5/5	100%	100%		
Right common trunk PV	1/1	1/1	100%	100%		
Right middle PV	2/2	2/2	100%	100%		
PV diameter						
		n	Enhanced MDCT	Non-enhanced MDCT	*P* value	Cumulative CV
LSPV	Antero-posterior	50	15.1 ± 4.2	15.5 ± 4.4	0.63	2.43
	Transverse	50	20.0 ± 3.3	20.4 ± 3.5	0.66	2.16
LIPV	Antero-posterior	50	12.9 ± 2.7	13.5 ± 2.8	0.60	2.37
	Transverse	50	17.8 ± 2.5	18.5 ± 2.5	0.50	2.05
RSPV	Antero-patriot	50	17.5 ± 3.8	18.4 ± 4.0	0.64	2.66
	Transverse	50	21.2 ± 3.5	21.5 ± 3.6	0.58	0.91
RIPV	Antero-posterior	50	14.0 ± 2.8	14.4 ± 2.9	0.60	1.86
	Transverse	50	17.6 ± 2.7	17.8 ± 2.7	0.95	1.07
Left common trunk PV ($n = 5$)	Antero-posterior	5	17.7 ± 5.4	18.1 ± 5.5	0.51	0.3
	Transverse	5	29.9 ± 2.6	30.5 ± 2.6	0.50	1.22
Right common trunk PV ($n = 1$)	Antero-posterior	1	18.7	19.1	–	1.06
	Transverse	1	26.8	26.9	–	0.09
RMPV ($n = 2$)	Antero-posterior	2	6.9, 7.5	7.2, 7.7	–	–
	Transverse	2	12.1, 11.5	12.4, 12.1	–	–

MDCT, multi-detector row computed tomography; PV, pulmonary vein; LSPV, left superior pulmonary vein; LIPV, left inferior pulmonary vein; RSPV, right superior pulmonary vein; RIPV, right inferior pulmonary vein; RMPV, right middle pulmonary artery; MDCT, multi-detector row computed tomography; CV, coefficient of variation.

the maximum local electrogram amplitude decreased by 70% or double potentials were noted. Irrigated RF ablation was performed 0.5–1.0 cm from the PV ostia, encircling the ipsilateral PV under NavX guidance. The endpoint of the extensive encircling PV isolation was defined as (i) elimination of PV potentials recorded by the two ring catheters within the ipsilateral PVs and lack of LA capture during intra-PV, isthmus, and PV atrium pacing at least 30 min after isolation and (ii) no recurrence of the PV spikes within all PVs after

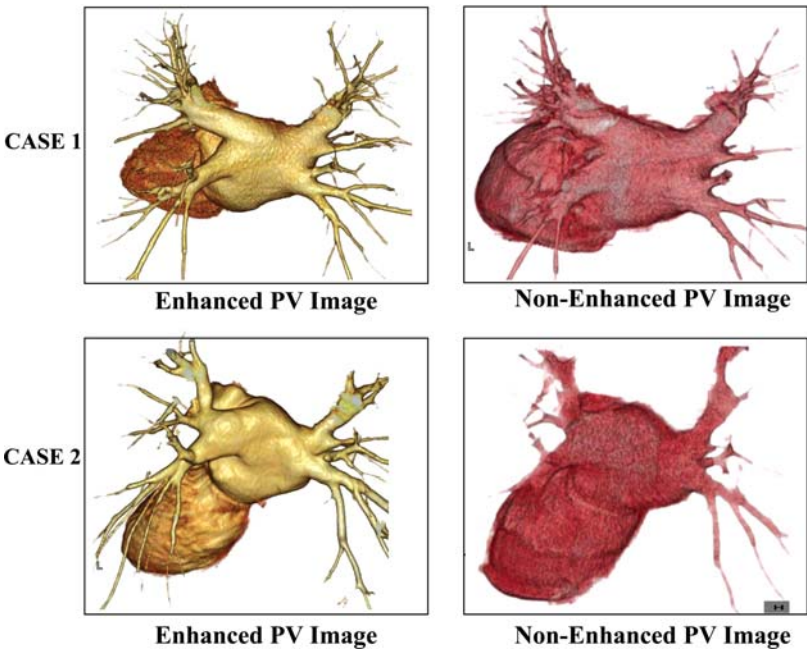

Figure 4 Comparison between non-enhanced and enhanced multi-detector row computed tomography images from a postero-anterior view. Acceptable agreement in gross anatomy between the two images was achieved.

intravenous administration of 20–40 mg of adenosine during sinus rhythm or coronary sinus pacing.

Post-ablation care and follow-up

After the procedure, intravenous heparin was administered for 2 days in all patients, followed by warfarin for at least 3 months. All patients were withdrawn from all previously ineffective antiarrhythmic drugs just after ablation. One day after the procedure, surface ECG, transthoracic echocardiography, and 24 h Holter recording were performed and repeated after 1, 3, and 6 months by our centre. All patients had a telemetry ECG recorder (Omron Co. Ltd., Kyoto, Japan) to document symptomatic arrhythmias or to transfer an ECG once per week if asymptomatic for 6 months.

Statistics

Bland–Altman plots were used for comparison of PV diameter between non-enhanced and enhanced MDCT images. Cumulative coefficients were used to evaluate differences in PV diameter between non-enhanced and enhanced MDCT images. Student's *t*-test was used to compare clinical characteristics, procedural parameters, and clinical outcomes between CKD patients who underwent PV isolation referring solely to non-enhanced MDCT images and non-CKD patients who underwent PV isolation with enhanced MDCT integrated with electroanatomic mapping. Data are expressed as the mean $\pm$ standard deviation (SD). Differences at $P < 0.05$ were considered statistically significant.

Results

For non-enhanced MDCT PV images, there were no differences in the detection of PV gross abnormalities between the two observers (*Table 2*, *Figure 4*). Similarly, complete agreement was obtained in the evaluation of PV gross anatomy between the two observers. Finally, no disagreement was observed in the PV gross anatomy between non-enhanced and enhanced MDCT image evaluations.

Pulmonary vein diameter measurements

Intra-observer differences in the PV diameter measurements of 50 sample PV images were <1 mm (mean $\pm$ SD, 0.1 ± 0.2 mm in non-enhanced MDCT; 0.3 ± 0.3 mm in enhanced MDCT) which were acceptably small. Similar results were obtained for inter-observers differences (0.1 ± 0.2 mm in non-enhanced MDCT; 0.2 ± 0.3 mm in enhanced MDCT). Brand–Altman plots showed acceptable agreement in PV diameter determinations between non-enhanced and enhanced MDCT PV images (*Figure 5*). The results of comparison of PV diameter determination between non-enhanced and enhanced images are summarized in *Table 2*. The cumulative coefficient of variation in PV diameter measurements was 0.91–2.66%, indicating good agreement in PV diameter measurements between non-enhanced and enhanced MDCT PV images.

Pulmonary vein isolation

Non-enhanced MDCT images could not be satisfactorily integrated with the electroanatomical maps. Therefore, for patients with CKD, the electroanatomical integration system could not be applied. Changes in the PV isolation catheter selected from non-enhanced MDCT image measurement was not required in any attempt in the CKD patients. *Table 3* summarizes the comparisons in procedural parameters and clinical outcomes between PV isolation for CKD patients referring solely to non-enhanced MDCT images and for non-CKD patients using the electroanatomical integration system with enhanced MDCT

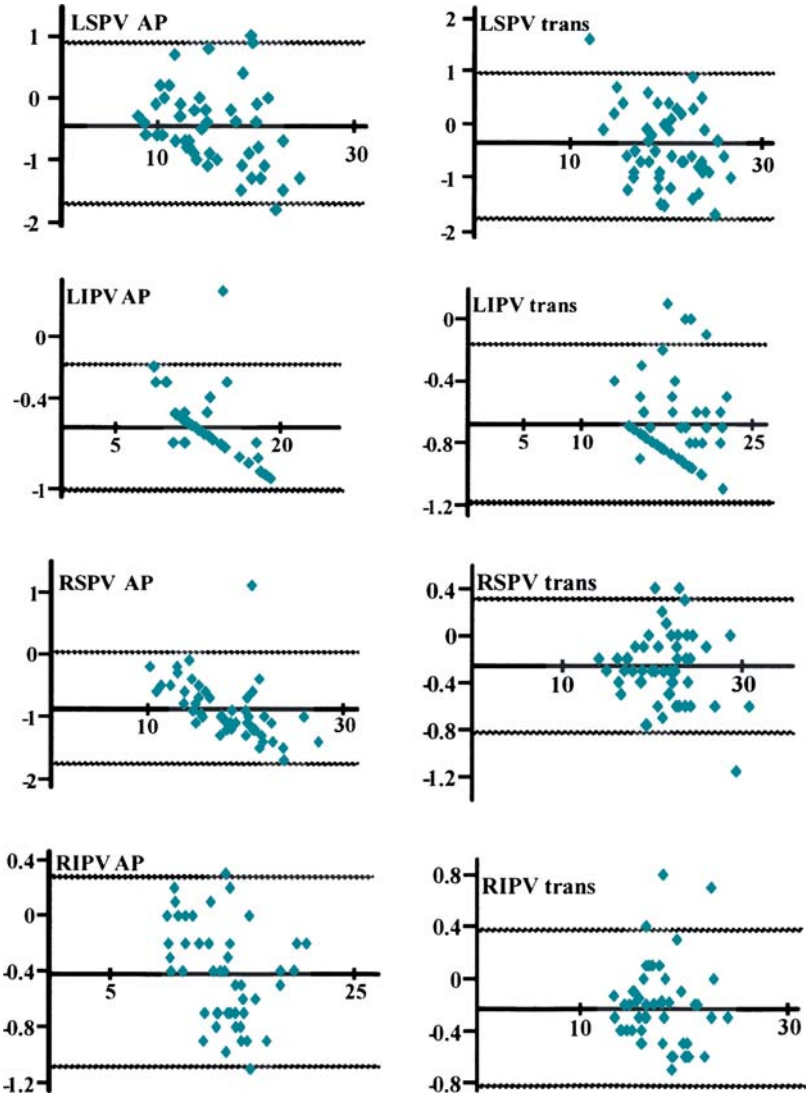

Figure 5 Bland–Altman plots for comparison of pulmonary vein diameter between non-enhanced and enhanced multi-detector row computed tomography images. LSPV, left superior pulmonary vein; LIPV, left inferior pulmonary vein; RSPV, right superior pulmonary vein; RIPV, right inferior pulmonary vein. AP, antero-posterior; trans, transverse.

images. There were no statistically significant differences in procedural or fluoroscopic times between PV isolation referring to non-enhanced MDCT and that by enhanced MDCT images integrated with an electroanatomical map. Similarly, the ablation success rate and AF free-status at 3 months after PV isolation did not differ between PV isolation using non-enhanced MDCT and that with the electroanatomical integration system. No complications occurred in PV isolation with or without enhanced MDCT.

Discussion

The present study has indicated for the first time that non-enhanced MDCT with a 64-detector row provides sufficient information regarding PV features and size for PV isolation in CKD patients with AF. There were no significant differences in procedural parameters and clinical outcomes between catheter ablation for AF referring only to non-enhanced MDCT images for CKD patients and that using electroanatomical integration systems with enhanced MDCT images for non-CKD patients.

To compare PV image dimensions between non-enhanced MDCT and enhanced MDCT, we used images obtained from the first preliminary non-enhanced MDCT in order to establish the conditions and settings for enhanced MDCT. The irradiation dose was not increased to make the comparisons in the present study, and the inter- and intra-observer differences in PV diameter measurements were acceptably small. Bland–Altman plots as well as the cumulative coefficient of variation were analysed to compare PV diameters obtained between non-enhanced and

Table 3 Comparisons between PV isolation for CKD(+) patients using solely non-enhanced multi-detector row computed tomography images and for CKD(−) patients using enhanced multi-detector row computed tomography images

	Group 1 ($n = 20$) CKD(+) group	Group 2 ($n = 30$) CKD(−) group	
PV 3D image	Non-enhanced MDCT	Enhanced MDCT	
Mapping system	NavX	NavX	
Procedure time (min)	134 ± 22	115 ± 18	0.99(NS)
Fluoroscopic time (min)	31 ± 9	25 ± 7	0.99(NS)
Ablation success (%)	100%	100%	NS
Complication (%)	0%	0%	NS
PV stenosis (>50%)	0%	0%	NS
AF free after 3 months (%)	75%	77%	NS

PV, pulmonary vein; CKD, chronic kidney disease; 3D, three dimensional; MDCT, multi-detector row computed tomography; AF, atrial fibrillation.

enhanced PV images. Based on the results of these careful analyses, the present study has demonstrated that non-enhanced PV images provide sufficient quantitative and qualitative PV morphological information for PV isolation.

Although the number of patients examined was small, the results indicate no notable differences in the procedural parameters and clinical outcomes between PV isolation referring solely to non-enhanced MDCT images and those using enhanced MDCT images integrated with an electroanatomical map. Our methods for catheter ablation for AF were essentially the same as recently described improved methods.[12,13] The fluoroscopic and procedural times in our PV isolation using an electroanatomical integration system with enhanced MDCT for patients without CKD were comparable to those in recent reports.[14,15] Further, our ablation success rate and AF free-status at 3 months for non-CKD patients were almost identical to recent studies.[13,15] Our results for procedural parameters and clinical outcome indicate that these methods for catheter ablation for AF are satisfactory. Furthermore, the clinical and echocardiographic parameters did not differ between the two groups, which validates any comparisons between the results.

There have been no previous reports regarding procedural parameters and clinical outcomes in catheter ablation with solely non-enhanced MDCT images for CKD patients, and thus the present results cannot be compared with reported results. Although the number of patients was relatively small, our results suggest that catheter ablation with non-enhanced MDCT images for CKD patients could be performed safely within a suitable time frame and with outcomes as successful as ablation using enhanced MDCT integrated with an electroanatomical map.

There are several possible reasons for the similar results between catheter ablation for AF referring to non-enhanced MDCT and those from enhanced MDCT images integrated with an electroanatomical map. First, ablation success determined by an electrophysiological endpoint was established in all patients. Second, accumulation of a certain amount of experience is thought to have enabled catheter ablation to be performed without an electroanatomical integration system with enhanced MDCT safely and within a suitable time frame to provide a successful outcome. Our results raise the question as to whether all catheter ablation for AF should be attempted with electrical mapping referring to non-enhanced MDCT. At present, it is not practically preferable to perform AF catheter ablation with non-enhanced MDCT because the ablation is much easier when using an electroanatomical integration system. However, the present results provide important information when considering reducing irradiation wherever possible, as even low-dose irradiation has carcinogenic potential.

Study limitation

One of the limitations of the present study was the relatively small number of CKD patients. However, the clinical and echocardiographic backgrounds were not different between the CKD and non-CKD groups, and very similar results were obtained between the two groups, suggesting that an increase in the number of patients is not likely to evoke different results.

Conclusions

Non-enhanced MDCT provides adequate PV image quality both quantitatively and qualitatively. Catheter ablation referring solely to non-enhanced MDCT images for AF seemed to provide clinically acceptable results in this small number of CKD patients. These findings warrant further studies involving a large number of patients to confirm the present results.

Conflict of interest: none declared.

References

1. Berkowitsch A, Greiss H, Vukajlovic D, Kuniss M, Neumann T, Zaltsberg S *et al.* Usefulness of atrial fibrillation burden as a predictor for success of pulmonary vein isolation. *Pacing Clin Electrophysiol* 2005;**28**:1292–301.
2. Macle L, Jais P, Weerasooriya R, Hocini M, Shah DC, Choi KJ *et al.* Irrigated-tip catheter ablation of pulmonary veins for treatment of atrial fibrillation. *J Cardiovasc Electrophysiol* 2002;**13**:1067–73.

3. Oral H, Knight BP, Tada H, Ozaydin M, Chugh A, Hassan S *et al.* Pulmonary vein isolation for paroxysmal and persistent atrial fibrillation. *Circulation* 2002;**105**:1077–81.
4. Tada H, Naito S, Kurosaki K, Ueda M, Ito S, Shinbo G *et al.* Segmental pulmonary vein isolation for paroxysmal atrial fibrillation improves quality of life and clinical outcomes. *Circ J* 2003;**67**:861–5.
5. Kumagai K, Noguchi H, Ogawa M, Nakashima H, Zhang B, Miura S *et al.* New approach to pulmonary vein isolation for atrial fibrillation using a multielectrode basket catheter. *Circ J* 2006;**70**:88–93.
6. Yamane T, Date T, Kanzaki Y, Inada K, Matsuo S, Shibayama K *et al.* Segmental pulmonary vein antrum isolation using the 'large-size' lasso catheter in patients with atrial fibrillation. *Circ J* 2007;**71**:753–60.
7. Monteiro MM, Saraiva C, Castelo Branco J, Cavaco D, Adragao P. Characterization of pulmonary vein morphology using multi-detector row CT study prior to radiofrequency ablation for atrial fibrillation. *Rev Port Cardiol* 2009;**28**:545–59.
8. Lacomis JM, Wigginton W, Fuhrman C, Schwartzman D, Armfield DR, Pealer KM. Multi-detector row CT of the left atrium and pulmonary veins before radiofrequency catheter ablation for atrial fibrillation. *Radiographics* 2003;**23**(Spec No):S35–48; discussion S-50.
9. Tang K, Ma J, Zhang S, Zhang JY, Wei YD, Chen YQ *et al.* A randomized prospective comparison of CartoMerge and CartoXP to guide circumferential pulmonary vein isolation for the treatment of paroxysmal atrial fibrillation. *Chin Med J (Engl)* 2008;**121**:508–12.
10. Kettering K, Greil GF, Fenchel M, Kramer U, Weig HJ, Busch M *et al.* Catheter ablation of atrial fibrillation using the Navx-/Ensite-system and a CT-/MRI-guided approach. *Clin Res Cardiol* 2009;**98**:285–96.
11. World Medical Association Declaration of Helsinki: Ethical principles for medical research involving human subjects. *JAMA* 2000;**284**:3043–5.
12. Jais P, Cauchemez B, Macle L, Daoud E, Khairy P, Subbiah R *et al.* Catheter ablation versus antiarrhythmic drugs for atrial fibrillation: the A4 study. *Circulation* 2008;**118**:2498–505.
13. Di Biase L, Elayi CS, Fahmy TS, Martin DO, Ching CK, Barrett C *et al.* Atrial fibrillation ablation strategies for paroxysmal patients: randomized comparison between different techniques. *Circ Arrhythm Electrophysiol* 2009;**2**:113–9.
14. Schmidt B, Tilz RR, Neven K, Julian Chun KR, Furnkranz A, Ouyang F. Remote robotic navigation and electroanatomical mapping for ablation of atrial fibrillation: considerations for navigation and impact on procedural outcome. *Circ Arrhythm Electrophysiol* 2009;**2**:120–8.
15. Rostock T, Steven D, Hoffmann B, Servatius H, Drewitz I, Sydow K *et al.* Chronic atrial fibrillation is a biatrial arrhythmia: data from catheter ablation of chronic atrial fibrillation aiming arrhythmia termination using a sequential ablation approach. *Circ Arrhythm Electrophysiol* 2008;**1**:344–53.